Analysis of Scattering Light from In-flight Particles in Suspension Plasma Spray for Size Measurement

A. Akbarnozari[1] · S. Amiri[1] · A. Dolatabadi[1] · C. Moreau[1]

Abstract Suspension plasma spray (SPS) is an emerging coating process for making surfaces with superior properties. In this process, in-flight spray particle characteristics such as size, velocity, and temperature have a direct influence on the properties of the deposited coatings. Accordingly, online diagnostic tools to characterize the in-flight particles in the SPS are sought by research laboratories and industrial centers for process optimization and control. However, small particle size, high temperature, and radiation of the plasma make it challenging to carry out these measurements. In this study, we used a light diffraction (LD) approach to measure online the size of in-flight particles sprayed from a well-predefined size distribution. Laser beam refraction by the hot plasma/gas jet is one of the main sources of noise for such size measurement. Successful measurements were achieved by shielding the measurement section and filtering the plasma radiation to reduce the influence of the laser refraction and plasma radiation. Results showed that the LD method has the potential to be used to monitor online the size distribution of in-flight particles in the SPS process.

Keywords diagnostic system · in-flight particle characterization · laser diffraction · light scattering · online measurement · particle size distribution · suspension plasma spray

✉ A. Akbarnozari
anozari007@gmail.com

[1] Concordia University, 1455 De Maisonneuve Blvd. W, Montreal H3G 1M8, Canada

Introduction

Suspension plasma spray (SPS) is a coating process in which feedstock particles of submicron size are introduced to high temperatures and high velocity plasma by a liquid carrier (Ref 1). As shown in Fig. 1, a plasma torch provides the heat and momentum to melt and direct the particles toward a substrate to produce a coating layer. In comparison, in atmospheric plasma spray (APS), the feed particles are around 10-100 μm in size and are injected into the plasma by a gas carrier. Undoubtedly, the use of finer particles in SPS compared to APS provides unique morphological, chemical, thermal, and mechanical properties to the SPS coatings (Ref 2-4). SPS coatings have been developed for a range of applications. For example, SPS has been studied by Jaworski et al. (Ref 5) for depositing hydroxyapatite coatings on biomaterial substrate. Thermal barrier coatings (TBC) for gas turbine blades were reviewed in works of Vassen et al. (Ref 6) and Fan et al. (Ref 7); in a more recent application, Sharifi et al. (Ref 8) sprayed titanium oxide to make a durable anti-icing surface for aircrafts; and finally, Aghasibeig et al. (Ref 9) produced an electrocatalytically active surface by SPS. Detailed description on the SPS process and its applications has been published in Ref 10, 11. Accordingly, the growing application of SPS requires a more precise understanding and control over the process which depends on capacity of diagnostic systems.

Particle Trajectory and Size Changes

Measuring particle size in the SPS process is particularly important as compared to APS process for two primary reasons: First, the trajectory of particles near the substrate depends on their size; second, particle size is prone to
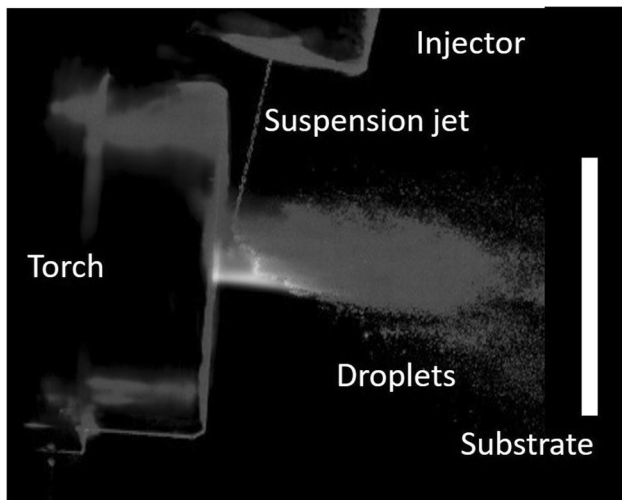
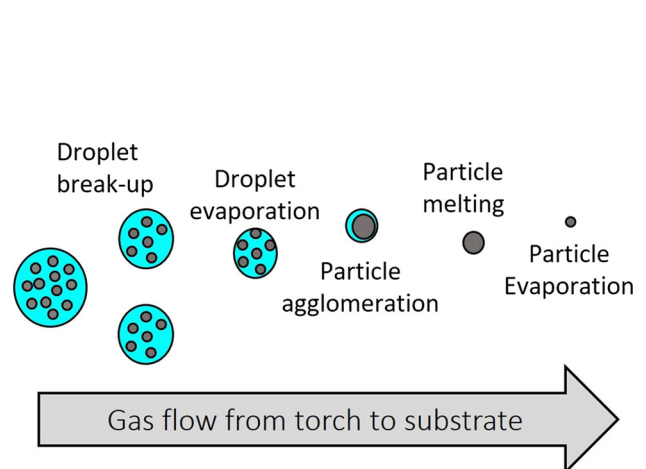Fig. 1 Suspension plasma process, the injection of suspension jet in the plasma and generating droplets

changes during the spray process. Berghaus et al. (Ref 12) modeled the velocity of particles near the substrate based on particle size. They noticed that both particle trajectory and velocity varied noticeably with size. Likewise, Crowe et al. (Ref 13) explained that particle trajectory depends on the interaction of particles with the containing gas quantified by Stokes number (St). St is defined as the ratio of the response time of the particle over the characteristic time of the flow. That is to say, for $St \ll 1$, a particle has sufficient time to respond to flow deviation, therefore following the fluid. This is the case for fine particles in spray when approaching the substrate. On the other hand, for the St 1 a particle does not have enough time to respond to the change of flow direction and therefore leaves the flow. The latter scenario corresponds to relatively larger particles, which get deposited on the substrate and contribute to
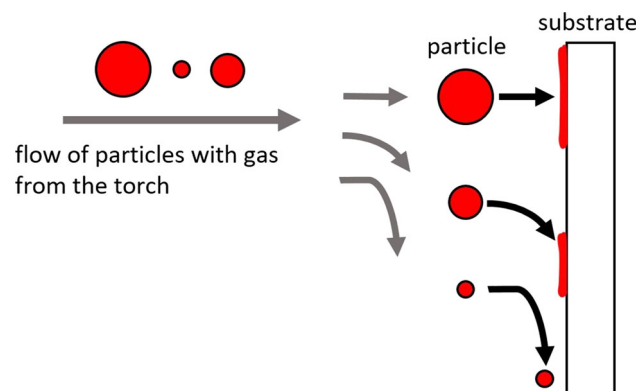
building the coating. Altogether, Fig. 2 shows schematically particle trajectories in terms of size near the substrate. This phenomenon has a strong influence on the coating microstructure and consequently coating properties. Additionally, VanEvery et al. (Ref 14) explained that when small particles moved almost parallel to the substrate, they stuck to asperities of the substrate surface or already deposited particles. This phenomenon, which causes the coating to have a columnar porous microstructure, has been named the shadow effect.

Pawlowski (Ref 15) described that particle size through the SPS process is prone to remarkable changes because of the agglomeration and evaporation of particles. Consequently, the size of particles close to the substrate is different from the size of feedstock particles. Figure 3 shows how the SPS process can cause changes in the size of particles. In this case, being exposed to plasma for a short time, the suspension jet interacted with the hot gas flow, breaking up into smaller droplets. The liquid phase of the suspension is then evaporated, and feedstock particles get closer to each other in droplets. At this time, adjacent particles start melting and get agglomerated in the heat of the process. On the other hand, the agglomerated and molten particles can undergo size decrease on their path toward the substrate because of evaporation. Therefore, the size of the in-flight particle near the substrate is not the same as the feedstock and depends on the actual spray conditions. In particular, Pourang et al. (Ref 16) modeled the SPS process and showed that, at a 6 cm standoff distance from the torch, the feedstock particles of a few hundred nanometers were agglomerated and formed particles averaging 1.0-1.5 μm in size. It is noteworthy to highlight that, throughout this paper, the word "droplet" is used to designate a droplet of atomized suspension, while the word "particle" designates a solid or molten particle of coating material as illustrated in Fig. 3.

Fig. 2 Schematic showing the effect of size on the trajectory of particles near the substrate. Large particles flow straight to the substrates, while very small particles deviate and move parallel to the substrate. Particles with intermediate size stay in between these two conditions

Fig. 3 Schematic showing the phenomena involved in the suspension plasma spray process

Online Measurement

Online monitoring of spray parameters is used in industry to control and guarantee the quality of deposited coatings and reduce the number of rejected parts (Ref 17). More than fifty parameters determine the actual plasma and injection conditions that affect the coating properties. Nonetheless, instead of monitoring each of these spray parameters, the characteristics of in-flight particles near the substrate can be monitored and provide the information required for adjusting the injection and plasma parameters. Fincke et al. (Ref 18) explained that supplying the result of online monitoring in a spraying process equipped by a real-time feedback control improves the repeatability, reliability, and reproducibility of coatings.

Diagnostic System

Fauchais et al. (Ref 19) reviewed the available diagnostic systems for thermal spray processes. Among the pioneers, Fincke et al. (Ref 20) measured size of particles from magnitude of scattered light. The first commercial diagnostic system for online characterization of in-flight particles was developed in the 1990s based on the works of Moreau et al. (Ref 21-26) and commercialized under the names DPV 2000 and DPV evolution (Tecnar, Saint-Bruno-de-Montarville, Canada). It measured the size, velocity, and temperature of in-flight particles in thermal spray processes. Then, Blain et al. (Ref 27) introduced an optical device that characterized online the particles during the APS process. Moreau et al. (Ref 28) explained how monitoring the spray process provided a tool to control coating properties in research centers and on the production floors. Moreover, Cetegen et al. (Ref 29) measured the size of the particles by phase Doppler particle anemometer (PDPA). In addition to optical method mentioned already, there were some researches to measure the size of in-flight particles through imaging techniques such as particle shape imaging (PSI) based on the works of Zimmermann et al. (Ref 30) and Landes (Ref 31). In another example, Wroblewski et al. (Ref 32) claimed to estimate the size of particles by using CCD arrays and applying topological criteria. In all available diagnostic systems except for PDPA, particles with a diameter larger than 5 μm were detectable (Ref 33) and fine particles of SPS were not able to be recognized. For a particular case, Rampon et al. (Ref 34) reported the use of a laser diffraction (LD) method to measure the droplet size of the YSZ suspension and the in-flight particles. Their results of size distribution are required to be validated.

The main objective of this study is to investigate the capabilities and limitations of the laser diffraction technique to measure online size distribution of in-flight particles in SPS process. To do so, approaches for reducing the influence of plasma radiation and laser refraction are discussed and implemented. Spray experiments were carried out with glass particles with a known particle size distribution to validate the online measurements.

## Theory and Background

Light Scattering

Particle size measurement by the light diffraction approach works based on Mie scattering theory, which states that the intensity of scattered light from a particle is a function of the particle size, shape, refractive index, wavelength, and polarization of incident light, and observation angle (scattering angle) (Ref 35). Figure 4 depicts a particle of radius a that received plane incident light of wavelength λ, and it scattered the intensity of I at scattering angle of θ. The scattering intensity was achieved from solving the equation of electromagnetic fields around the particle (Ref 36), and it is represented by Stokes matrix. For scattering of a spherical particle from receiving an unpolarized beam of incident light, the Stokes parameters are given in Eq 1:

$$I_s = S_{11}I_i \quad Q_s = S_{12}I_i \quad U_s = V_s = 0, \qquad \text{(Eq 1)}$$

where I_s represents scattering intensity, Q_s and U_s show linear polarization, and V_s shows circular polarization. I_i is the incident light, and S_{11} and S_{12} are elements of Stokes parameters matrix which are calculated by Eq 2:

$$S_{11} = \frac{1}{2}\left(|S_2|^2 + |S_1|^2\right) \quad S_{12} = \frac{1}{2}\left(|S_2|^2 - |S_1|^2\right). \qquad \text{(Eq 2)}$$

And S_1 and S_2 are elements of the amplitude scattering matrix which are calculated through Eq 3:
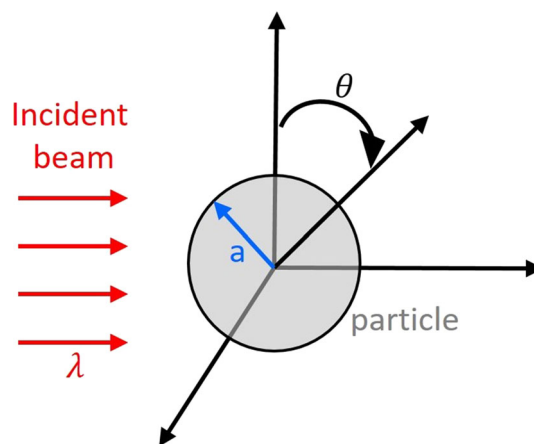
Fig. 4 Polar coordination for studying scattering of a spherical particle of radius r exposed incident beam of wavelength λ

$$S_1(\theta) = \sum_{n=1}^{\infty} \frac{2n+1}{n(n+1)} [a_n \pi_n + b_n \tau_n]$$

$$S_2(\theta) = \sum_{n=1}^{\infty} \frac{2n+1}{n(n+1)} [a_n \tau_n + b_n \pi_n]. \quad \text{(Eq 3)}$$

In this equation, a_n and b_n are scattering coefficients and π_n and τ_n are angle-dependent functions given in Eq 4 and 5:

$$a_n = \frac{m\psi_n(mx)\psi_n'(x) - \psi_n'(mx)\psi_n(x)}{m\psi_n(mx)\xi_n'(x) - \psi_n'(mx)\xi_n(x)}$$

$$b_n = \frac{\psi_n(mx)\psi_n'(x) - m\psi_n'(mx)\psi_n(x)}{\psi_n(mx)\xi_n'(x) - m\psi_n'(mx)\xi_n(x)} \quad \text{(Eq 4)}$$

$$\pi_n(\cos\theta) = \frac{1}{\sin\theta} P_n^1(\cos\theta)$$

$$\tau_n(\cos\theta) = -\sin\theta \frac{P_n^1(\cos\theta)}{d(\cos\theta)}, \quad \text{(Eq 5)}$$

where ψ_n and ξ_n are Riccati–Bessel functions and P_n is Legendre polynomials. x and m are the size parameter and relative refractive index, respectively, as are shown in Eq 6 and 7:

$$x = \frac{2\pi na}{\lambda} \quad \text{(Eq 6)}$$

$$m = \frac{n_1}{n}, \quad \text{(Eq 7)}$$

where n and n_1 are the refractive indices of medium and particle, respectively. All equations illustrate how the scattering intensity (I) is related to the size of particle (a). For example, Fig. 5 shows the scattering intensity from a laser beam at $\lambda = 633$ nm by water droplets of 1, 4, and 10 μm in air. The scattering intensity is maximum at 0°; however, it reduces up to 90° and afterward it increases again. The changes in scattering intensity as a function of angle reduce as the size of the particles decreases.

Size of the particles is calculated from scattering intensity by solving an inversion problem (Ref 37, 38). In brief, the inversion problem starts by assuming a size distribution for the particles and calculates the scattering intensity for that distribution. In the second step, the calculated scattering intensity was compared with the experimentally acquired scattering intensity to correct the assumed size distribution. Iteration of correcting the size distribution and calculating the scattering intensity leads to find the particle size distribution. The inversion problem finds size distribution of particles for a known wavelength and given scattering intensity at a scattering angle. Substantially, the smaller particles mainly scatter light in a wide angle, while the larger particles mainly scatter light in a low angle (close to 0°). Although this method is well established, the SPS process introduced some challenges to be overcome. Mainly, the refraction of laser beams, plasma light, and minimum number of particles in the measurement volume were investigated in this study.
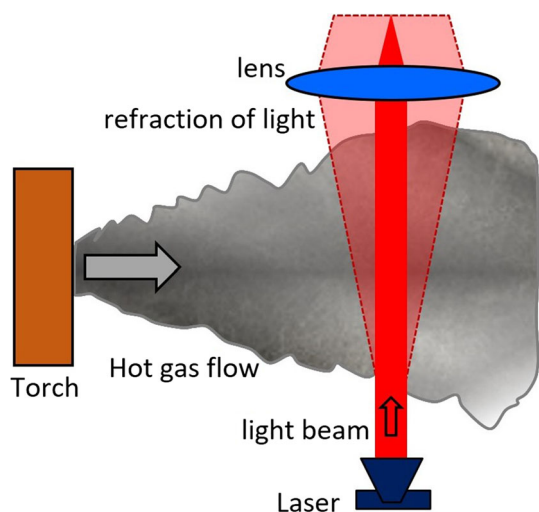
Laser Beam Refraction

Laser beam refraction means bending of light because of a change in the speed of light when the light goes across a medium. Fundamentally, a ray of light deviates when it leaves a medium of index of refraction n_0 and enters a different medium of index n_1. In this case, the angle of deviation is proportional to the ratio of refractive indices of two media. For a mixture of media (fluids), the refractive index of the mixture is a function of the refractive indices and volume fractions of pure components. In addition, refractive index depends on density, temperature, and temperature gradient of media (Ref 39-41). Therefore, light refraction (beam steering) occurs when the medium of measurement is not uniform with respect to temperature, density, or composition. For example, Dumouchel et al. (Ref 42) investigated the laser beam steering in a spray and they reported that the beam steering caused overestimation of size distribution for drops.

Figure 6 illustrates schematically the beam steering when it passed through a hot gas. In other words, the gas in the measurement section was composed of several

Fig. 5 Scattering intensity as a function of angle and size around a spherical droplet
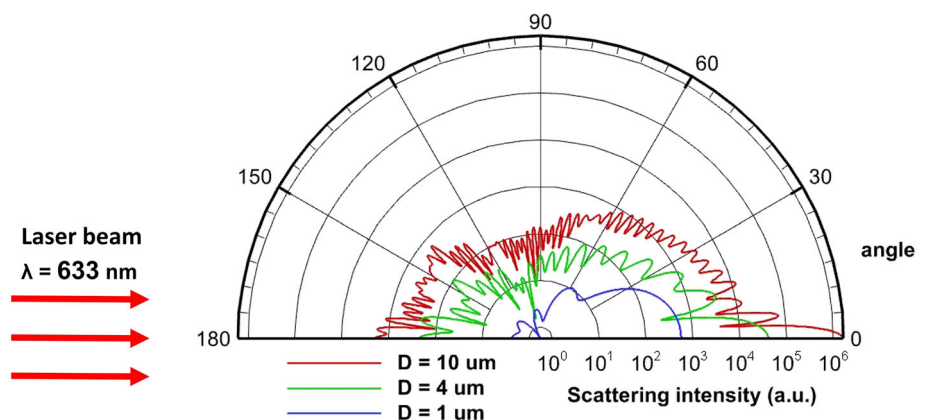
Fig. 6 Laser beam steering, laser light refraction in the plasma and defocusing unscattered laser

elements, hot gases (typically a mixture of neutral gases such as argon and/or helium, or combustion produces like CO and/or CO_2), and the surrounding cold air with different volume fractions. When the hot gas gets mixed with the cool surrounding air in the turbulent flow, the mixture of the two gases did not have uniform temperature and density distributions. Therefore, the laser beam is refracted in a small angle and it does not have the so-called unperturbed trajectory. In other words, the figure schematically shows that instead of a sharp-tip red cone of light that meets in 0°, the light is spread like a truncated light red cone in angles of around 1°.

Plasma Light

Plasma has radiation in a range from infrared to ultraviolet. The radiation of plasma is reflected from the surfaces and is refracted by the particles that exist around the plasma. The radiation of plasma is measured by a spectrometer at different distances for different ranges of wavelengths. Seeing that, Gougeon et al. (Ref 43) and Aziz et al. (Ref 44) reported the plasma radiation in the range of visible and infrared wavelengths for plasma spray process. Plasma radiation causes some challenges to use optical diagnostic devices in the plasma spray process. Therefore, it is necessary to prevent or minimize the effect of plasma radiation and reflection on detectors of the optical diagnostic system. Using a shield and bandpass filter minimizes the effect of plasma on the system.

Number of Particles

Success measurement depended on capturing signals from an adequate number of particles in measurement volume.

Specifically, the small size of the target particles was one of the main measurement challenges in this study. In the extreme case of Mie scattering (close to the geometrical optics), when the ratio of particle size to the incident light wavelength is more than 10, the intensity of scattered signal by a particle changes proportional to a^2 where a is the radius (Ref 45). Generally, this ratio varies between $0.55a^2$ and $1.90a^2$ in the region of Mie scattering. Therefore, as the size of particles in the SPS process reduces around one order of magnitude compared to APS process, the intensity of their scattered signal reduces between 55 and 190 times. Therefore, a minimum number of particles should present in the measurement volume to scatter enough stable light to stimulate the detector for a correct size distribution.

Experimental Methodology

Material

The testing material for the size measurement was glass particles (Cospheric, USA). The micrograph and size distribution of particles are illustrated in Fig. 7, which confirms median size (D_{v50}) of 4 μm. There were several reasons for selecting this material: (i) Its size distribution was quite close to the range of particle sizes which were expected to be observed near the substrate during the SPS process, (ii) it had a narrow size distribution, (iii) in terms of safety, it was neither toxic nor hazardous, and (iv) it was suspended in the water uniformly and did not agglomerate or sediment during preparation or injection. The particles were soda lime glass microspheres with an index of refraction 1.5 as specified by the supplier. Test of glass particles made it possible to perform the test of online size measurement and, more importantly, to validate the result. To prepare suspension, 10 wt.% glass particles were mixed with distilled water by a mechanical stirrer and an ultrasonic liquid mixer (QSonica, USA) to have a homogeneous suspension.

Plasma and Injection System

Figure 8 shows the plasma spray and the suspension injection systems. In detail, the suspension was injected to the hot gas flow by a homemade injection system composed of a pressurized suspension tank equipped with agitating device, a Coriolis flow meter, and an injector. The plasma torch was 3 MB fed by argon gas with a flow rate of 60 SLPM and the plasma power around 16 kW. The suspension was injected at 60 mL/min (mLPM) from an orifice of 250 μm. Size of the in-flight particles was measured at a standoff distance of 20 cm from the torch on the
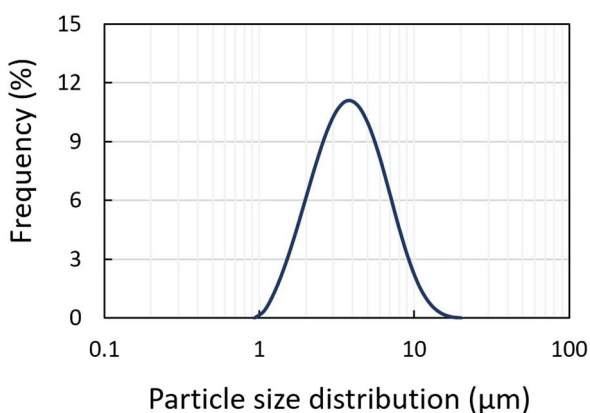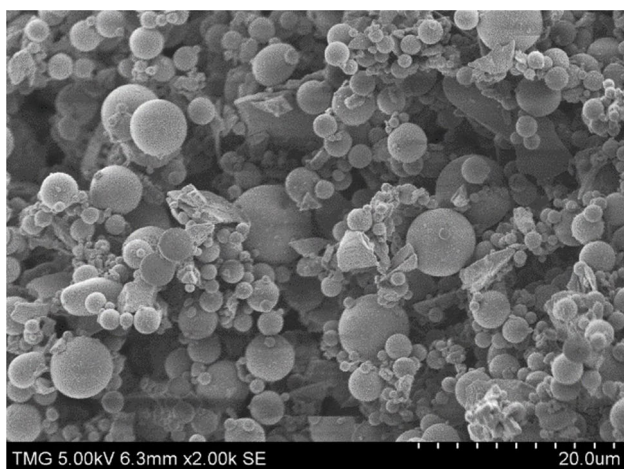
Fig. 7 SEM microstructure of the glass particles (top) and their particle size distribution (bottom)
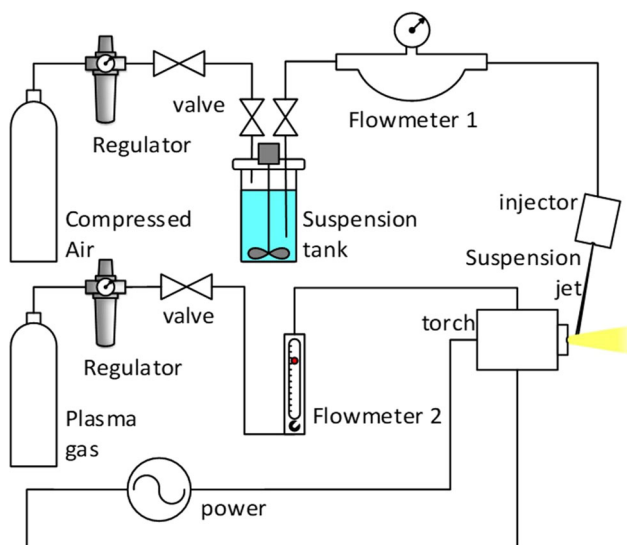
Fig. 8 Plasma spray and suspension injection systems

centerline of plasma. The effect of plasma radiation and light on measurement was reduced at 20 cm of the torch.

This distance was more than usual spray condition which is between 4 and 6 cm. However, the size of in-flight particles does not change after 6 cm. By measurement at 20 cm, the size was the same as 6 cm and the effect of plasma noise was reduced. Choice of plasma conditions (such as argon gas and relatively low plasma power) and injection conditions was adjusted to prevent from melting and changing the size of the glass particles during the spray. Therefore, the result of online measurement could be validated by comparing with the size distribution of the feedstock particles. In other words, it was expected that the particle size distribution of the in-flight particles would be the same as particle size distribution of the feedstock material.

Acquisition Apparatus

Diagnostic system was Spraytec (Malvern Panalytical, Grovewood, UK) which functioned based on the Mie scattering and was first introduced by Swithenbank et al. (Ref 46). It had two configurations to characterize the samples: first, for a spray of particles in air used for online measurement; second, for the particles circulated in a liquid of a closed-loop system (wet dispersion unit). The latter configuration was used for offline measurement to validate the result and also to find the minimum number of particles. The diagnostic system had a helium neon laser of 2 mW at a wavelength of 633 nm and with a beam diameter of 10 mm. Moreover, its detector consisted of 36 concentric silicon diode array sensors situated between 0° and 18° where detector zero was at zero angle and detector 36 was at the angle of 18° of unscattered laser. The data acquisition rate of the system was between 1000 Hz and 10 kHz. Also, effective range of size measurement for the system was 0.1-1000 μm. For measurement, the LD system captured background and raw signals. The background was obtained with the plasma and laser and without particles. The raw signal was obtained with plasma, laser, and particles. Finally, it calculated the scattering intensity of particles by subtraction the background signal from the raw signal. Briefly, the scattering intensity of the in-flight particles is calculated from Eq 8:

$$I_p = I_{RS} - I_{BG}, \tag{Eq 8}$$

where I_p, I_{RS}, and I_{BG} are scattering light intensity of particles, raw intensity, and background light intensity, respectively. In SPS, the background was expressed as the measured intensity when the plasma was running and pure water (no suspension) was injected. In the same way, the raw intensity was declared a measured intensity when plasma was running at the time suspension was injected. Figure 9 shows the configuration of the diagnostic system in the SPS process, including the measurement section,
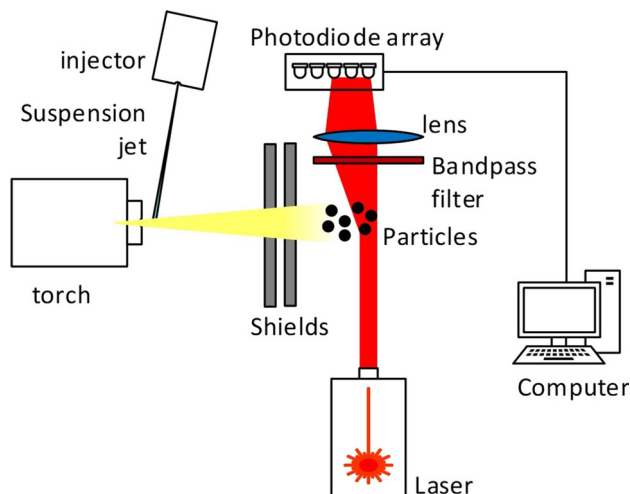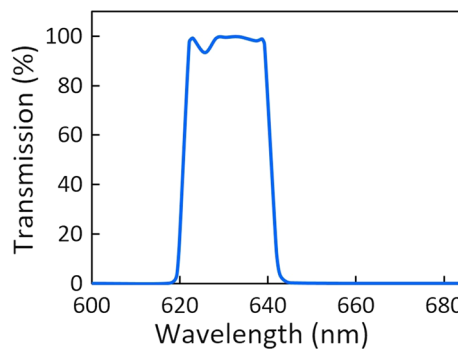
Fig. 9 Schematics of test setup composed of a suspension injection, a plasma torch, and laser diffraction systems; two layers of shields were placed between the torch and the diagnostic system

laser, and the detector, two layers of shields, and bandpass filter. The emitted plasma light was prevented from reaching the detectors by the shields and a bandpass filter. For shielding, a plate of steel with an aperture of a few millimeters was placed in front of the torch. The size of aperture was optimized through experiments. A second shield from aluminum with an aperture of 10 mm was placed after the first shield to prevent the heat transfer of hot steel to the measurement volume and to direct the flow of gas through the laser of the diagnostic system. The deployment of the shields was for research studies; however, it could be replaced with a more practical configuration which is currently under development in our laboratory.

Although the shield in the test setup blocked direct radiation from the plasma to the detectors, the reflected radiation from the spray booth reached the detectors. Under these circumstances, the bandpass filter, with transmission around the wavelength of the laser, was mounted in front of the detectors to eliminate the plasma light. Equally important, the range of transmissions of the selected filter was wide enough to accept tilted incident scattering after the blueshift. Figure 10 illustrates that the filter had a transmission between 626 and 640 nm. Besides, for wavelengths less than 600 and more than 680 nm, the transmission was negligible.

Scattering of particles from the plasma was eliminated for the measurement. In reality, the filter permitted the spectrum, within transmission range, to reach the detector regardless of the source of radiation. The particles scattered light from two sources: first, the laser light of the diagnostic system; second, the radiation of the plasma. To understand the impact of these scattering signals on measurement, the irradiance of a particle distribution from

these two sources was calculated based on MiePlot's (Philip Laven) Mie theory. For this purpose, the scattering of glass particles with D_{50} of 4 μm and a standard deviation of 50% (similar to the testing powder) were studied. Figure 11 shows the calculation of the irradiance of the particles from laser sources compared to the calculated irradiance of a particle from plasma at spray distances of 4 cm (typical SPS standoff distance and without any bandpass filter in the diagnostic system) and 20 cm (suggested standoff distance for this study) with and without the bandpass filter. Altogether, the graph reveals that particle light scattering from plasma and laser was in the same order of magnitude at the spray distance of 4 cm without the filter. By using the filter and measurement in 20 cm, the scattered plasma reduced three orders of magnitudes compared to the scattered laser. Thus, using the bandpass

Fig. 10 Transmission range of the bandpass filter for the detector
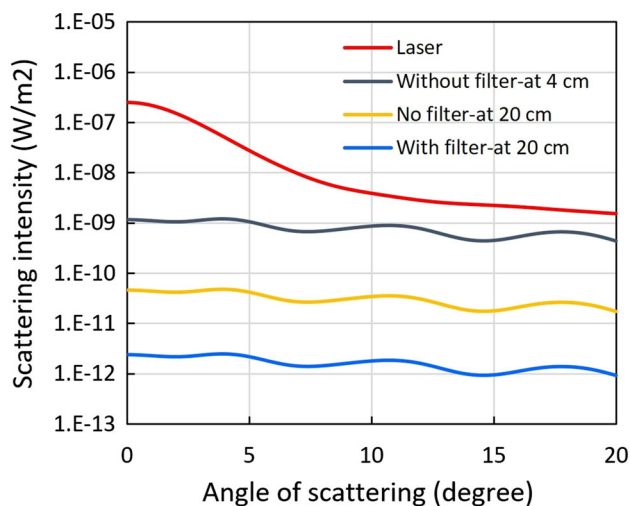
Fig. 11 Calculated scattering intensity based on Mie theory for glass particles with a lognormal distribution around an average size of 4 μm and standard deviation of 50%, from a laser source at a wavelength of 633 nm (red line), from a source of plasma at standoff distance of 4 cm without any filter (gray line), from the source of plasma at standoff distance of 20 cm without any filter (orange line), and from the source of plasma at standoff distance of 20 cm with a bandpass filter of 626-640 nm (blue line) (Color figure online)

filter for the detector and adjusting the measurement volume in right distance from the torch minimized the effect of scattered plasma. Technically speaking, calculated scattering intensity by particles from the plasma source shows effect of filtering to reduce noise.

Results and Discussion

Minimum Number of Particles

Practically, in SPS, the number of particles was mainly controlled by the concentration of powder in suspension and the flow rate of injection. In this study, the minimum number of particles was measured from doing a set of experiments at the wet dispersion unit. According to the experiment, there was no measurable signal at a lower number of particles in the measurement volume. By adding more particles, scattering intensity became stable and size was measured correctly for the given particles. For the glass powder with an average diameter of 4 μm, the minimum number of particles was around 15,000, which corresponded to the peak intensity of 40 (a.u.) in the graph of scattering signal versus the detector. LD system calculates particle size distribution when ensemble measurement of scattering signals from all the particles in the measurement volume was above a minimum level of light intensity defined based on the sensor specification. Moreover, number density of particles and size of measurement volume experienced a constant change during the spray because of plasma condition and suspension injection. Therefore, the number of particles in measurement volume was a key parameter insured the response of the system for reliable measurement. Generally, the scattering intensity corresponded to the signal of the glass particles when the majority of water droplets were vaporized by adjusting the plasma power. However, the presence of the water droplets in the measurement volume had an impact on the raw signal. Ideally, the diagnostic system measured the size of in-flight particle when the liquid droplets fully evaporated. As one step in the SPS process, the liquid phase of suspension droplets was vaporized during their residence time in the hot gas. This step was mainly controlled by adjusting the power of the plasma system and injection conditions. Although the existence of droplets in measurement volume was inevitable because of the instabilities of both plasma and injection during spray, it is necessary to understand the possible effect of the droplet signal on the measurement. For example, Marchand et al. (Ref 47) measured the droplet size for superpulsating atomization, where D_{50} was around 20 μm. In our case, the irradiance of water droplets of this size was calculated and compared with the irradiance of glass particles with D_{50} of 4 μm and standard

deviation of 47%. Figure 12 reveals that the irradiance for a water droplet at their peak was equaled the irradiance of 56 particles. Moreover, calculations showed that the irradiance of one water droplet was around 12 times more than the irradiance of one particle in the angle of peak intensity of the particle (detectors 27 and 28). In other words, the scattering of one droplet was equivalent to the scattering of 12 particles. Therefore, the number of particles must be sufficiently more than the number of droplets to have reliable signal for particle size measurement. The calculations showed that the presence of water droplets in the measurement volume results a bimodal graph. In our experiment, the measurement illustrated the scattering signal was unimodal and the peak belonged to the signal from the in-flight particles. This meant the number of droplets in the measurement section was quite low and it did not interfere in the measurement of particle size.

Influence of the Shields

Refraction of light caused that the laser was received in several detectors near the zero angle without scattering from any particles. This led to extensive light intensity in the background and the raw signal in the first detectors because of refraction in small angles. Figure 13 depicts the effect of the beam steering on the background intensity received in all detectors by comparing three measurement conditions: when the plasma was not running (the blue triangle), when the plasma was running without a shield (red circle), and finally, when the plasma was running and the shields were placed between the torch and the diagnostic system. In our experiment, refraction was within an angle of less than 1°; nevertheless, it was large enough to influence the first twelve detectors to different extents
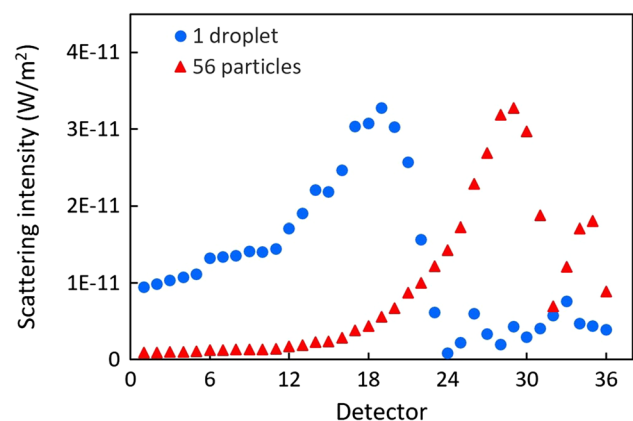
Fig. 12 Calculated scattering intensity of one water droplet with an average size of 20 μm and standard deviation of 50%, compared to scattering intensity of 56 glass particles with average size of 4 μm and standard deviation of 50% to assess possible effect of droplets on the scattering signal
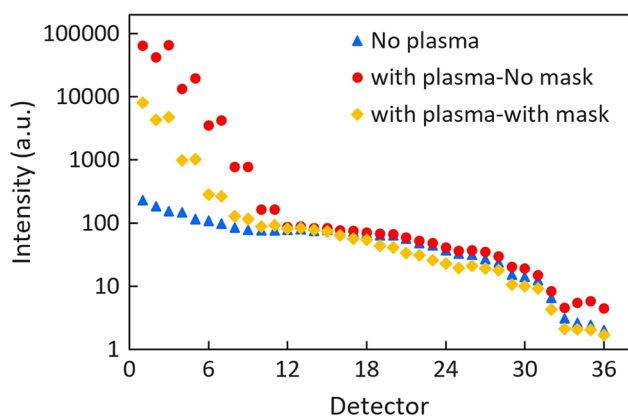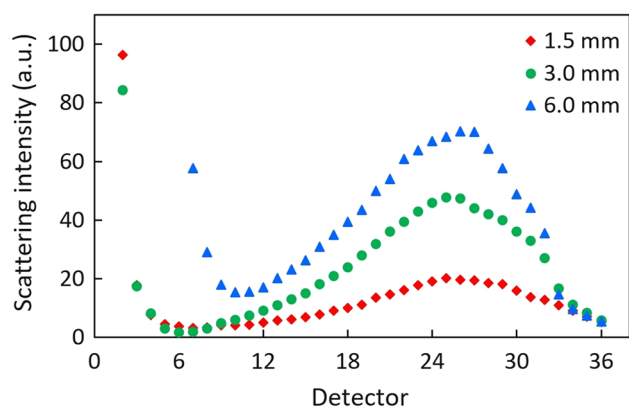
Fig. 13 Experimentally measured background light on detectors: no plasma (blue triangles); plasma without shields (red circles); plasma with shields (orange rhombuses) (Color figure online)

Fig. 14 Effect of aperture size of the shield on received scattering intensity by the particles in the detectors

depending on spray conditions. Under the experiment circumstance, the intensity of the signal in the first twelve detectors for the plasma condition was three orders of magnitude greater than the time the plasma was off. The effects of laser refraction were partially eliminated from the background and the raw signal by mounting the shields between the torch and the diagnostic system. In comparison, the shields reduced the background signal for plasma by at least one order of magnitude in the first detectors. From detector 12 to the last one, there were no significant differences between measurements of background for three cases. In brief, experimentally measured background light shows the effect of plasma on diagnostic system when there were no particles to scatter light from plasma and laser.

The shields had an aperture to transfer of gas from the torch to the measurement volume. The effect of the aperture size of front shield was studied in terms of light scattering. The size of aperture controlled the flow rate of particle-contained hot gas passing through the test section. Of course, the aperture size had dual effects: on the scattering intensity of the particles and on the refraction of the laser beam in the measurement section. Figure 14 shows the scattering intensity of particles for the aperture sizes of 1.5, 3.0, and 6.0 mm, which were measured under optimum spray conditions. The scattering intensity was minimum around the detector 11, and it was maximum around detectors 27 and 28 which correspond to glass particles of 4 μm for all the cases. Generally, if the number density of the particles was uniform when the diameter aperture was doubled, the scattering intensity should have increased four times. Comparison of result of three apertures confirmed that the particles were not distributed uniformly in the spray. As an example, the peak of the intensity increased from around 25-50 (a.u.) when the aperture size changed from 1.5-3.0 mm. Particularly, it was

observed that the scattered intensity did not elevate to more than 75 (a.u.) when the orifice size increased to 6.0 mm. Therefore, the number density of particles at the center of the plume was greater than the number density at the periphery. Consequently, by increasing the diameter of the aperture, the average of number density of particles all over the measurement section reduced. Moreover, the diameter of the laser beam was finite to 10 mm and a larger aperture did not introduce any more particles in the measurement volume.

Besides the fact that the aperture size impacted the total scattering intensity of particles, it also modified the temperature and temperature gradient of the gas in the measurement volume. The temperature was raised as aperture size was increased. As a result, a high temperature and temperature gradient caused the laser beam to refract, which consequently generated superfluous intensity in the first detectors. Altogether, it was helpful to optimize the system by maximizing the scattering signal while minimizing refraction. For this ambivalent effect of the aperture size on the measurement, the optimum size was specified in terms of SNR which was defined as the ratio of raw signals
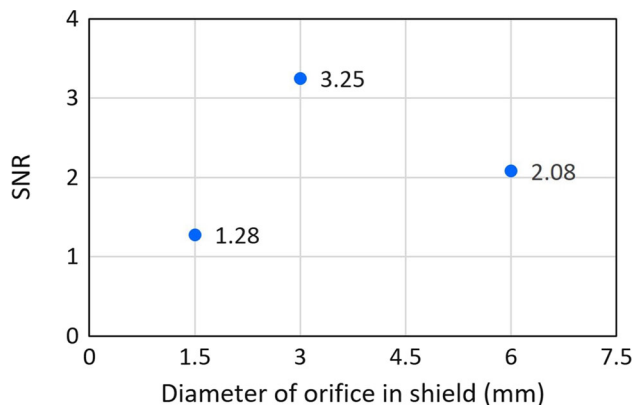
Fig. 15 Signal-to-noise ratio (SNR) for three aperture sizes of the shield

from particles over the background. Figure 15 shows SNR for three aperture sizes at the detectors 27 and 28 where the peak of scattering intensity for glass particles was situated. SNR was the highest for the middle size aperture (3.0 mm), and it was around 3.25. Two statements were suggested for this observation: First, the 3.0-mm aperture limited the amount of hot gas that changed the temperature in measurement volume and consequently reduced the noise; second, the width of a cylinder of hot gas in the measurement volume was smaller and, respectively, the light refraction was less.

Time-Resolved Measurement

The stability of the scattering intensity by in-flight particles was accessed through a time-resolved measurement acquired at 10 kHz. Figure 16 presents the scattering intensity at detectors 1, 11, and 28. The signal fluctuated noticeably in the detector 1, and the signal fluctuation in the next detectors was reduced gradually. The signal in detector 11 shows almost no significant fluctuation. The scattering intensity from detector 11 to detector 28, which was the position of scattering peak, showed stable result. To find the origin of fluctuations, the Fourier transform (FT) of the signal was acquired. Analysis of FT result confirmed that there was not any distinct frequency associated with the range of plasma fluctuations which expected to be between 2 and 6 kHz (Ref 48, 49). A possible source of low-frequency fluctuations was the turbulence flow and gas instability at the measurement volume.

Figure 17 indicates the scattering signal of particles in the detectors under the two conditions of plasma spray and wet dispersion unit. In comparison, both curves mostly showed the same trend; however, there were some discrepancies in the first and last detectors. In fact, the temperature gradient of gas mixture caused laser light to deviate, which was the source of the discrepancy in the first

detectors. Besides, the medium of measurement was the air for the test of plasma spray and water for the test of wet dispersion unit. The index of refraction of air and water is 1.00 and 1.33, respectively. The calculation for a same particle size distribution in the two media illustrated that the scattering intensity in the water was more than the scattering intensity in the air in the angle where the last detectors were situated. Therefore, using the different media for the measurement was reason for the slight difference between the curves for the detectors from 30 to 36.

The particle size distributions extracted from these scattering signals are shown in Fig. 18. It is remarkable that D_{50} measured in the plasma spray and wet dispersion unit was 4.7 and 4.6 μm, respectively. Accordingly, the difference of D_{50} under two conditions was 3.4%. The minimum particle size in two measurements was around 0.8 μm, and the maximum particle size for in-flight and feedstock particles was 17.1 and 14.7 μm, respectively. Overall, the size distribution measured in the plasma condition and the wet dispersion unit were nearly identical. This result confirmed that the LD system measured size of in-flight particles correctly under the plasma condition. The accuracy and precision of measurement by the LD system are both better than 1% according to the manufacturer.

The particles are assumed spherical in the LD system, and all the calculations to find particle size distribution are based on this assumption. The feedstock powders for SPS processes are mostly nonspherical. However, they become molten in the plasma and form spherical shape when they move toward the substrate. Therefore, in SPS, spherical particles present in the measurement volume. For the cases that the nonspherical particles would be in the measurement volume, the scattered light does not represent the particle thoroughly and the size distribution would be a rough estimation of the reality.

Fig. 16 Scattering intensity sampled at 10 kHz in detector number 1 (green line, scaled at left axis), detector number 11 (blue line), and detector number 28 (red line, both scaled at the right axis) (Color figure online)
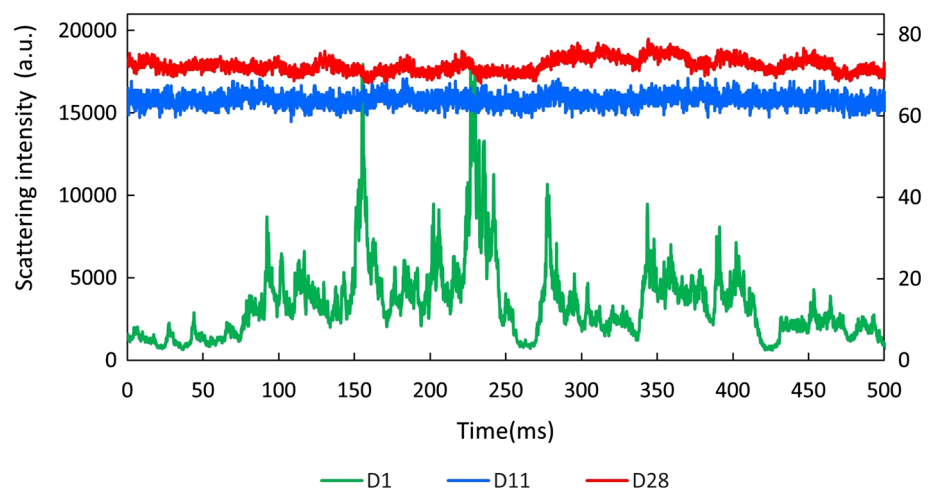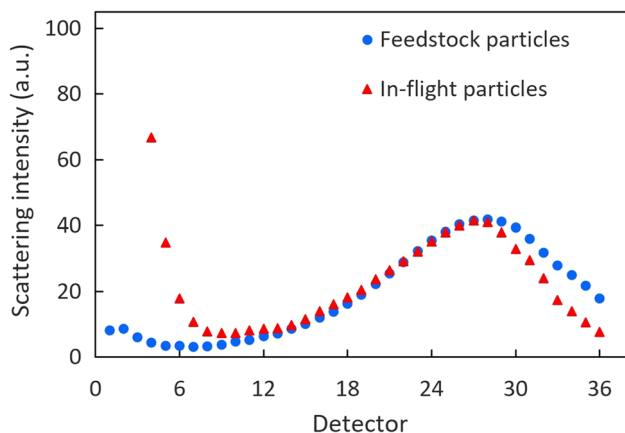
Fig. 17 Scattering intensity of glass particles (feedstock powder in the wet dispersion unit) compared to scattering intensity of the in-flight particles in plasma spray when the particles were not melted
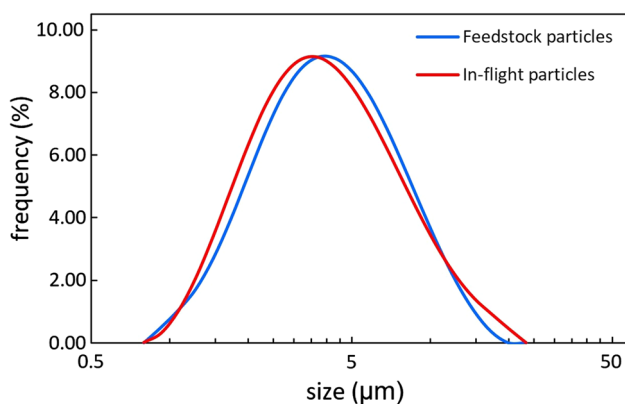
Fig. 18 Particle size distribution of glass particles (feedstock powder in the wet dispersion unit) compared to particle size distribution of the in-flight particles in plasma spray when the particles were not melted

Conclusions

In this study, the light diffraction method was used to measure online the size of the in-flight particles in SPS process; (i) the shields effectively controlled the number of particles and refraction in the measurement volume, (ii) the size of apertures in the front shield was optimized in terms of SNR, (iii) the plasma radiation from surrounding and scattered plasma by particles in the measurement volume was reduced to a negligible value compared to the scattered light from the laser of the diagnostic system, (iv) the minimum number of particles needed to collect the required scattering signal was identified for the coating material, (v) the monomodal scattering intensity verified that there is no droplet available in the measurement zone, and finally (vi) a comparison of size distribution in the plasma condition with the wet dispersion unit showed consistency between the size distribution of feedstock and in-flight particles.

It was concluded that the LD method has the potential to be applied for the online size measurement of the in-flight particles in the SPS process. However, to eliminate the effect of plasma from the measurement signal was quite challenging which still require more investigation. It is necessary to develop a protocol to validate the result of online measurement, especially for smaller particles, and the spray condition for the industrial coating powders.

References

1. J. Tucker and C. Robert, *ASM Handbook*, Vol 5A, Thermal Spray Technology ASM International, Materials Park, 2013
2. P. Fauchais, G. Montavon, R. Lima, and B. Marple, Engineering a New Class of Thermal Spray Nano-Based Microstructures from Agglomerated Nanostructured Particles, Suspensions and Solutions: An Invited Review, *J. Phys. D*, 2011, **44**, p 093001
3. H. Kassner, R. Siegert, D. Hathiramani, R. Vassen, and D. Stoever, Application of Suspension Plasma Spraying (SPS) for Manufacture Of Ceramic Coatings, *J. Therm. Spray Technol.*, 2008, **17**, p 115-123
4. A. Vardelle, C. Moreau, J. Akedo, H. Ashrafizadeh, C.C. Berndt, J.O. Berghaus, M. Boulos, J. Brogan, A.C. Bourtsalas, and A. Dolatabadi, The Thermal Spray Roadmap, *J. Therm. Spray Technol.*, 2016, **2016**, p 1-65
5. R. Jaworski, L. Pawlowski, C. Pierlot, F. Roudet, S. Kozerski, and F. Petit, Recent Developments in Suspension Plasma Sprayed Titanium Oxide and Hydroxyapatite Coatings, *J. Therm. Spray Technol.*, 2010, **19**, p 240-247
6. R. Vaßen, M.O. Jarligo, T. Steinke, D.E. Mack, and D. Stöver, Overview on Advanced Thermal Barrier Coatings, *Surf. Coat. Technol.*, 2010, **205**, p 938-942
7. W. Fan and Y. Bai, Review of Suspension and Solution Precursor Plasma Sprayed Thermal Barrier Coatings, *Ceram. Int.*, 2016, **42**, p 14299-14312
8. N. Sharifi, M. Pugh, C. Moreau, and A. Dolatabadi, Developing Hydrophobic and Superhydrophobic TiO$_2$ Coatings by Plasma Spraying, *Surf. Coat. Technol.*, 2016, **289**, p 29-36
9. M. Aghasibeig, C. Moreau, A. Dolatabadi, and R. Wuthrich, Fabrication of Nickel Electrode Coatings by Combination of Atmospheric and Suspension Plasma Spray Processes, *Surf. Coat. Technol.*, 2016, **285**, p 68-76
10. A. Killinger, R. Gadow, G. Mauer, A. Guignard, R. Vaßen, and D. Stöver, Review of New Developments in Suspension and Solution Precursor Thermal Spray Processes, *J. Therm. Spray Technol.*, 2011, **20**, p 677
11. P. Fauchais, M. Vardelle, and S. Goutier, Latest Researches Advances of Plasma Spraying: From Splat to Coating Formation, *J. Therm. Spray Technol.*, 2016, **25**, p 1534-1553
12. J.O. Berghaus, S. Bouaricha, J.G. Legoux, and C. Moreau, Injection Conditions and In-flight Particle States in Suspension Plasma Spraying of Alumina and Zirconia Nano-Ceramics, in *Thermal Spray 2005: Thermal Spray Connects: Explore Its Surfacing Potential! (DVS-ASM)*, 2005, p 2-7
13. C.T. Crowe, *Multiphase Flow Handbook*, CRC Press, London, 2005

14. K. VanEvery, M.J. Krane, R.W. Trice, H. Wang, W. Porter, M. Besser, D. Sordelet, J. Ilavsky, and J. Almer, Column Formation in Suspension Plasma-Sprayed Coatings and Resultant Thermal Properties, *J. Therm. Spray Technol.*, 2011, **20**, p 817-828

15. L. Pawlowski, Suspension and solution thermal spray coatings, *Surf. Coat. Technol.*, 2009, **203**, p 2807-2829

16. K. Pourang, C. Moreau, and A. Dolatabadi, Effect of Substrate and Its Shape on In-flight Particle Characteristics in Suspension Plasma Spraying, *J. Therm. Spray Technol.*, 2016, **25**, p 44-54

17. P. Fauchais and M. Vardelle, Sensors in spray processes, *J. Therm. Spray Technol.*, 2010, **19**, p 668-694

18. J.R. Fincke, W.D. Swank, R.L. Bewley, D.C. Haggard, M. Gevelber, and D. Wroblewski, Diagnostics and Control in the Thermal Spray Process, *Surf. Coat. Technol.*, 2001, **146**, p 537-543

19. P.L. Fauchais, J.V. Heberlein, and M.I. Boulos, *Thermal Spray Fundamentals: From Powder to Part*, Springer, Berlin, 2014

20. J. Fincke, C. Jeffery, and S. Englert, In-flight Measurement of Particle Size and Temperature, *J. Phys. E Sci. Instrum.*, 1988, **21**, p 367

21. C. Moreau and M. Lamontagne, Method and Apparatus for Monitoring the Temperature and Velocity of Plasma Sprayed Particles. Patent No. 5,180,921, 1993

22. P. Gougeon, C. Moreau, V. Lacasse, M. Lamontagne, I. Powell, and A. Bewsher, A new Sensor for On-Line Diagnostics of Particles Under Thermal Spraying Conditions, in *Advanced Processing Techniques*, ed. by C. Lall and A. J. Neupaver, International Conference on Powder Metallurgy and Particulate Materials, Toronto, Canada, Metal Powder Industries Federation, APMI, 1994, p 199-210

23. P. Gougeon, C. Moreau, and F. Richard. On-Line control of plasma sprayed particles in the Aerospace industry, in *Advances in Thermal Spray Science and Technology*, ed. by C.C. Berndt and S. Sampath. Proceedings of the National Thermal Spray Conference, Houston, Texas, ASM International, 1995, p 149-155

24. C. Moreau, P. Gougeon, A. Burgess, and D. Ross. Characterization of Particle Flows in an Axial Injection Plasma Torch, in *Advances in Thermal Spray Science and Technology*, ed. by C.C. Berndt and S. Sampath, Proceedings of the National Thermal Spray Conference, Houston, Texas, ASM International, 1995, p 141-147

25. C. Moreau, P. Gougeon, and M. Lamontagne, Method and Apparatus for Monitoring the Diameter of thermally Sprayed Particles. Patent No. 5,654797, 1997

26. C. Moreau, P. Gougeon, M. Lamontagne, V. Lacasse, G. Vaudreuil, and P. Cielo, On-Line Control of the Plasma Spraying Process by Monitoring the Temperature, Velocity, and Trajectory of In-flight Particles, in *Thermal Spray Industrial Applications*, ed. by C.C. Berndt and S. Sampath, Proceedings of the National Thermal Spray Conference, 20-24 June 1994, Boston, Mass., ASM International, 1994, p 431-437.

27. J. Blain, F. Nadeau, L. Pouliot, C. Moreau, P. Gougeon, and L. Leblanc, Integrated infrared sensor system for on line monitoring of thermally sprayed particles, *Surf. Eng.*, 1997, **13**, p 420-424

28. C. Moreau, J. Bisson, R. Lima, and B. Marple, Diagnostics for Advanced Materials Processing by Plasma Spraying, *Pure Appl. Chem.*, 2005, **77**, p 443-462

29. B. Cetegen and W. Yu, In-situ Particle Temperature, Velocity, and Size Measurements in dc Arc Plasma Thermal Sprays, *J. Therm. Spray Technol.*, 1999, **8**, p 57-67

30. S. Zimmermann and K. Landes, A Particle Image Shape Imaging (PSI) Investigation of Particles in a Plasma Jet, *Mater. Sci. Eng. A*, 2004, **383**, p 153-157

31. K. Landes, Diagnostics in Plasma Spraying Techniques, *Surf. Coat. Technol.*, 2006, **201**, p 1948-1954

32. D. Wroblewski, G. Reimann, M. Tuttle, D. Radgowski, M. Cannamela, S. Basu, and M. Gevelber, Sensor Issues and Requirements for Developing Real-Time Control for Plasma Spray Deposition, *J. Therm. Spray Technol.*, 2010, **19**, p 723-735

33. A. Killinger, P. Müller, and R. Gadow, What Do We Know, What are the Current Limitations of Suspension HVOF Spraying?, *J. Therm. Spray Technol.*, 2015, **24**, p 1130–1142

34. R. Rampon, O. Marchand, C. Filiatre, and G. Bertrand, Influence of Suspension Characteristics on Coatings Microstructure Obtained by Suspension Plasma Spraying, *Surf. Coat. Technol.*, 2008, **202**, p 4337-4342

35. M. Bass, E.W. Van Stryland, D.R. Williams, and W. Wolfe, *Handbook of Optics Fundamentals, Techniques, and Design*, Vol I, Optical Society of America, Washington, 1995

36. C.F. Bohren and D.R. Huffman, *Absorption and Scattering of Light by Small Particles*, Wiley, New York, 2008

37. T. Igushi and H. Yoshida, Influence of the Number of Detectors by Laser Scattering Method for Estimation of Particle Size, *Rev. Sci. Instrum.*, 2012, **83**, p 055103

38. L.P. Bayvel, J. Knight, and G. Robertson, Alternative Model-Independent Inversion Programme for Malvern Particle Sizer, *Part. Part. Syst. Charact.*, 1987, **4**, p 49-53

39. J.C. Owens, Optical Refractive Index of Air: Dependence on Pressure, Temperature and Composition, *Appl. Opt.*, 1967, **6**, p 51-59

40. L. Zhang, J. Petit, and J. Taine, Measurements of Temperature Profiles in Gases by Laser Beam Deflection, *Rev. Phys. Appl.*, 1989, **24**, p 401-410

41. C. Innocenti and A. Consortini, Refractive Index Gradient of the Atmosphere at Near Ground Levels, *J. Mod. Opt.*, 2005, **52**, p 671-689

42. C. Dumouchel, P. Yongyingsakthavorn, and J. Cousin, Light Multiple Scattering Correction of Laser-Diffraction Spray Drop-Size Distribution Measurements, *Int. J. Multiph. Flow*, 2009, **35**, p 277-287

43. P. Gougeon and C. Moreau, In-flight Particle Surface Temperature Measurement: Influence of the Plasma Light Scattered by the Particles, *J. Therm. Spray Technol.*, 1993, **2**, p 229-233

44. B. Aziz, P. Gougeon, and C. Moreau, Temperature Measurement Challenges and limitations for in-flight Particles in Suspension Plasma Spraying, *J. Therm. Spray Technol.*, 2017, **26**, p 695-707

45. I.S. Merrill, *Introduction to Radar Systems*, Mc Grow-Hill, New York, 2001, p 607-609

46. J. Swithenbank, J. M. Beer, D. S. Taylor, D. Abbot, and G. C. McCreath. A Laser Diagnostic Technique for the Measurement of Droplet and Particle Size Distribution, in *AIAA 14th Aerospace Sciences Meeting*, Washington, D.C., 1976, p 69-76

47. O. Marchand, L. Girardot, M. Planche, P. Bertrand, Y. Bailly, and G. Bertrand, An Insight into Suspension Plasma Spray: Injection of the Suspension and Its Interaction with the Plasma Flow, *J. Therm. Spray Technol.*, 2011, **20**, p 1310-1320

48. R. Etchart-Salas, V. Rat, J. Coudert, P. Fauchais, N. Caron, K. Wittman, and S. Alexandre, Influence of Plasma Instabilities in Ceramic Suspension Plasma Spraying, *J. Therm. Spray Technol.*, 2007, **16**, p 857-865

49. J. Bisson, B. Gauthier, and C. Moreau, Effect of Plasma Fluctuations on In-flight Particle Parameters, *J. Therm. Spray Technol.*, 2003, **12**, p 38-43